Available online at www.sciencedirect.com
SCIENCE DIRECT®
Journal of Sound and Vibration 284 (2005) 283–298
JOURNAL OF SOUND AND VIBRATION
www.elsevier.com/locate/jsvi

Acoustic performance of a Herschel–Quincke tube modified with an interconnecting pipe

J.M. Desantes, A.J. Torregrosa*, H. Climent, D. Moya

CMT—Motores Térmicos, Universidad Politécnica de Valencia, Camino de Vera s/n, 46022 Valencia, Spain

Received 15 September 2003; received in revised form 10 June 2004; accepted 15 June 2004
Available online 10 November 2004

Abstract

The classical two-duct Herschel–Quincke tube is modified by means of an additional pipe connecting both paths. A transfer matrix is obtained for a mesh system with five arbitrary branches and then particularized to the proposed scheme. Experimental attenuation measurements were performed on several prototypes, and the results compared favourably with predictions from the previous theoretical development. Finally, transmission loss contour plots were used to study the influence of the connecting pipe on the resonance frequencies. The results confirm the nontrivial character of the influence observed, and simple relationships are obtained for the general trends.

1. Introduction

The Herschel–Quincke (H–Q) tube is a simple implementation of the interference principle in an acoustic attenuation device: two ducts of arbitrary length and section (within reasonable limits) in a parallel arrangement. Herschel [1] first discussed the idea of acoustic interference of musical tones in such a system. He predicted that cancellation of tones would occur when the difference in path length between the recombined signals divided by the wavelength of the acoustic wave was a series of constant values. Some years later, Quincke's experiments [2] demonstrated that Herschel's system did effectively cancel sound. A thorough study of the acoustics of H–Q tubes

*Corresponding author. Tel.: +34-963-877-658; fax: +34-963-877-659.
E-mail address: atorreg@mot.upv.es (A.J. Torregrosa).

0022-460X/$ - see front matter © 2004 Elsevier Ltd. All rights reserved.
doi:10.1016/j.jsv.2004.06.016

was presented by Selamet et al. [3], indicating that, when the classical restriction to equal cross section for both ducts is removed, the attenuation obtained is not limited to narrow spikes, and hence it is interesting even for automotive exhaust applications, as an alternative to other resonant devices, such as concentric resonators. This is supported by the fact that numerous patents have been proposed which are based on the two-duct or the multiple-duct configurations. A list of these patents may be found in Ref. [4], as well as a complete study of the multiple-duct H–Q tube.

Considering the application of H–Q tubes to systems such as compressors and the intake and exhaust systems of internal combustion engines, the effect of a mean flow is not negligible. Several attempts to extend one-dimensional theory to this case have been reported, for a single HQ tube [5] and also for a double-stage HQ tube [6], assuming the usual decoupling between the mean flow and the acoustic field.

In this paper, a modification of the usual H–Q tube is considered, in which an additional duct connecting both branches is included; apart from increasing the number of design variables, this configuration is representative of an imperfect separation of the interfering paths in practical implementations of the interference principle as those cited in Ref. [4]. As a first approximation, a one-dimensional acoustic solution with no mean flow is developed.

The paper consists of five sections: following this introduction, the closed-form expression for the transfer matrix of the modified H–Q tube is developed. Then, this theoretical development is validated by comparison with experimental results of the transmission loss. Next, attenuation spikes of the transmission loss computed from the transfer matrix obtained are investigated in order to get a global view of the connecting pipe influence as well as the main tendencies in the acoustic behaviour of the system. The study is concluded with some final observations.

2. Theory

A general expression is available [7] for the transfer matrix of a system consisting of an arbitrary number of subsystems connected in parallel or in series. However, when there are interconnections between these subsystems a general expression cannot be found, and thus a specific expression must be devised for each case.

The modified H–Q tube, as considered in this work, is a particular case of a system consisting of five arbitrary branches, connected as shown in Fig. 1. Location 1 represents the inlet to the whole system, while locations 2 and 3 represent the inlet of the two interfering paths corresponding to a simple H–Q tube; each of these is divided into two branches, labelled 1 and 4 for the first path and 2 and 5 for the second one, while branch 3 represents the interconnecting pipe. Then, locations 4

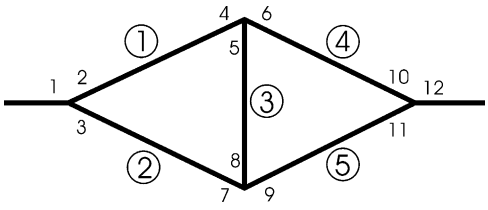

Fig. 1. A general interferential system with interconnecting branch.

(outlet of branch 1), 6 (inlet to branch 4) and 5 (top endpoint of branch 3) correspond to the junction of the interconnecting pipe with the first interfering path, while locations 7 (outlet of branch 2), 9 (inlet to branch 5) and 8 (bottom endpoint of branch 3) represent the junction of the interconnecting pipe with the second interfering path. Finally, locations 10 and 11 represent the outlet of the two interfering paths associated with a simple H–Q tube, and location 12 is the outlet of the whole system. Assuming one-dimensional propagation, each branch is characterized by its transfer matrix. Denote the transfer matrix of the jth branch as $\mathbf{T}_j$, with

$$\mathbf{T}_j = \begin{bmatrix} A_j & B_j \\ C_j & D_j \end{bmatrix}, \quad j = 1, 2, \ldots, 5. \tag{1}$$

Then, according to the notation described above, the state variables at the two endpoints of each branch are related by

$$\begin{bmatrix} p_2 \\ v_2 \end{bmatrix} = \begin{bmatrix} A_1 & B_1 \\ C_1 & D_1 \end{bmatrix} \cdot \begin{bmatrix} p_4 \\ v_4 \end{bmatrix}, \quad \begin{bmatrix} p_3 \\ v_3 \end{bmatrix} = \begin{bmatrix} A_2 & B_2 \\ C_2 & D_2 \end{bmatrix} \cdot \begin{bmatrix} p_7 \\ v_7 \end{bmatrix}, \quad \begin{bmatrix} p_5 \\ v_5 \end{bmatrix} = \begin{bmatrix} A_3 & B_3 \\ C_3 & D_3 \end{bmatrix} \cdot \begin{bmatrix} p_8 \\ v_8 \end{bmatrix},$$
$$\begin{bmatrix} p_6 \\ v_6 \end{bmatrix} = \begin{bmatrix} A_4 & B_4 \\ C_4 & D_4 \end{bmatrix} \cdot \begin{bmatrix} p_{10} \\ v_{10} \end{bmatrix}, \quad \begin{bmatrix} p_9 \\ v_9 \end{bmatrix} = \begin{bmatrix} A_5 & B_5 \\ C_5 & D_5 \end{bmatrix} \cdot \begin{bmatrix} p_{11} \\ v_{11} \end{bmatrix}, \tag{2}$$

where p is the pressure fluctuation and v is the mass flow rate fluctuation. Now, continuity of pressure and mass flow rate fluctuations at the junctions gives

$$\begin{aligned} &p_1 = p_2 = p_3, \quad p_4 = p_5 = p_6, \quad p_7 = p_8 = p_9, \quad p_{10} = p_{11} = p_{12}, \\ &v_1 = v_2 + v_3, \quad v_4 = v_5 + v_6, \quad v_7 + v_8 = v_9, \quad v_{10} + v_{11} = v_{12}. \end{aligned} \tag{3}$$

Since no mean flow is being considered, all the elements used are reciprocal and hence the determinants of their transfer matrices are equal to unity [8]. Then, solving simultaneously Eqs. (2) and (3) yields

$$\begin{aligned} mp_1 - nv_1 &= tp_{12} + B_4 v_{12}, \\ xp_1 + yv_1 &= zp_{12} + D_4 v_{12}, \end{aligned} \tag{4}$$

where only p_{12} and v_{12} are unknowns; the coefficients in Eq. (4) are given by

$$\begin{aligned} m &= e - \frac{bf}{c}, \quad n = d + \frac{af}{c}, \quad t = g + \frac{f}{B_5 c}, \\ x &= h + \frac{bk}{c}, \quad y = \frac{ak}{c} - i, \quad z = j - \frac{k}{B_5 c}. \end{aligned} \tag{5}$$

Here,

$$a = A_2 + B_2\left(\frac{D_5}{B_5} + \frac{A_3}{B_3}\right), \quad b = \frac{D_1}{B_3} - C_2 - D_2\left(\frac{D_5}{B_5} + \frac{A_3}{B_3}\right),$$

$$c = \frac{B_1}{B_3} + A_2 + B_2\left(\frac{D_5}{B_5} + \frac{A_3}{B_3}\right), \quad d = \frac{B_4 B_2}{B_5}, \quad e = D_1 + \frac{B_4 D_2}{B_5},$$
$$f = B_1 - \frac{B_4 B_2}{B_5}, \quad g = A_4 + \frac{B_4 A_5}{B_5}, \quad h = \frac{D_2}{B_3} - C_1 + \frac{D_4 D_2}{B_5} - \frac{D_3 D_1}{B_3},$$
$$i = \frac{B_2}{B_3} + \frac{D_4 B_2}{B_5}, \quad j = C_4 + \frac{D_4 A_5}{B_5}, \quad k = \frac{D_4 B_2}{B_5} + \frac{B_2}{B_3} + \frac{D_3 B_1}{B_3} + A_1. \tag{6}$$

Now, Eq. (4) may be rewritten as a transfer matrix equation as follows:

$$\begin{bmatrix} p_1 \\ v_1 \end{bmatrix} = \begin{bmatrix} \dfrac{ty + nz}{xn + ym} & \dfrac{B_4 y + nD_4}{xn + ym} \\ \dfrac{zm - xt}{xn + ym} & \dfrac{D_4 m - xB_4}{xn + ym} \end{bmatrix} \begin{bmatrix} p_{12} \\ v_{12} \end{bmatrix}. \tag{7}$$

In order to check this general expression for the transfer matrix, some well-known limiting cases are considered. From Fig. 1, it is clear that if the connecting branch collapses to a single point, the result should correspond to two simple interferential systems connected in series, whereas blocking wave transmission through this branch would result in a single interferential system. In the appendix it is verified that Eq. (7) reduces to the corresponding transfer matrices found in the literature in both limiting cases.

Once this consistency check is done, the H–Q tube with an interconnecting pipe may be addressed. It is assumed that all branches are now uniform ducts, this is, straight ducts of constant cross section. The transfer matrix of a duct of cross section S_j and length L_j without mean flow may be written as [9]

$$[T_{\text{duct}}]_j = \frac{1}{2\alpha_j} \begin{bmatrix} \phi_j & a_0/S_j \\ S_j/a_0 & \phi_j \end{bmatrix}. \tag{8}$$

Here, a_0 is the speed of sound, and ϕ_j and α_j are defined as

$$\phi_j = \frac{1 + e^{-2ikL_j}}{1 - e^{-2ikL_j}}, \quad \alpha_j = \frac{e^{-ikL_j}}{1 - e^{-2ikL_j}}, \tag{9}$$

where i is the imaginary unit and $k = \omega/a_0$ is the wave number. Substitution of Eq. (8) into Eq. (6) gives

$$a = \frac{1}{2\alpha_2}\left(\phi_2 + \frac{\phi_5 S_5 + \phi_3 S_3}{S_2}\right), \quad b = \frac{\phi_1 \alpha_3 S_3}{\alpha_1 a_0} - \frac{\phi_2}{2\alpha_2 a_0}\left(\frac{S_2}{\phi_2} + \phi_5 S_5 + \phi_3 S_3\right),$$
$$c = \frac{S_3 \alpha_3}{S_1 \alpha_1} + \frac{1}{2\alpha_2}\left(\phi_2 + \frac{\phi_5 S_5 + \phi_3 S_3}{S_2}\right), \quad d = \frac{a_0 S_5 \alpha_5}{2 S_2 \alpha_2 S_4 \alpha_4}, \quad e = \frac{1}{2}\left(\frac{\phi_1}{\alpha_1} + \frac{\phi_2 S_5 \alpha_5}{\alpha_2 S_4 \alpha_4}\right),$$
$$f = \frac{a_0}{2}\left(\frac{1}{\alpha_1 S_1} - \frac{S_5 \alpha_5}{S_2 \alpha_2 S_4 \alpha_4}\right), \quad g = \frac{1}{2\alpha_4}\left(\phi_4 + \frac{S_5 \phi_5}{S_4}\right),$$

$$h = \frac{\phi_2}{a_0\alpha_2}\left(S_3\alpha_3 + \frac{\phi_4 S_5\alpha_5}{2\alpha_4}\right) - \frac{S_1 + \phi_1 S_3\phi_3}{2a_0\alpha_1}, \quad i = \frac{1}{S_2\alpha_2}\left(S_3\alpha_3 + \frac{\phi_4 S_5\alpha_5}{2\alpha_4}\right),$$
$$j = \frac{S_4 + \phi_4 S_5\phi_5}{2a_0\alpha_4}, \quad k = \frac{1}{S_2\alpha_2}\left(S_3\alpha_3 + \frac{\phi_4 S_5\alpha_5}{2\alpha_4}\right) + \frac{1}{2\alpha_1}\left(\phi_1 + \frac{S_3\phi_3}{S_1}\right). \tag{10}$$

Then, from Eqs. (5) and (7) the transfer matrix may be written explicitly.

3. Experimental work

In order to validate the expression obtained for the modified H–Q tube, several prototypes were built with the same structure, but with different duct lengths. For simplicity, all duct diameters were equal, except in the case of the interconnecting pipe, which was varied. A simple representation of one of these prototypes is given in Fig. 2; each of the five relevant ducts was flanked by two of the existing four junctions. All the prototypes were built with commercial PVC ducts and junctions.

Measurements were carried out with a modified impulse method [10] in order to obtain the acoustic characteristics of the prototypes. An example of the direct comparison between the transmission loss (TL) measurements and the results computed with the transfer matrix obtained from Eqs. (5) and (10) is given in Fig. 3. The case considered is precisely that shown in Fig. 2; the three straight pipes were of the same length, $L_1 = L_3 = L_4 = L$, whereas the two bended ducts were longer, $L_2 = L_5 = \frac{9}{5}L$, with $L = 240$ mm. The TL is plotted as a function of the nondimensional frequency $f(L_1 + L_4)/a_0$, where f is the frequency and a_0, as above, is the speed of sound. This comparison reveals that, at least for nondimensional frequencies below 1, the calculation reproduces all the essential features found in the measurement. However, some deviations are observed. Apart from small dissipative and flow effects, unavoidable with the measurement technique used [10], two main sources of discrepancy are considered: (i) the description of the duct junctions and (ii) the assumption that all ducts are straight, whereas some of the ducts in the prototype are bended. Regarding the first point, the commercial T junctions used in the prototype are quite complex, incorporating some area changes, and it is to be expected that some three-dimensional effects appear at high frequencies; obviously, the consideration of the junctions as nondimensional elements cannot account for such effects. Regarding the effect of duct curvature, three-dimensional effects are also to be expected at relatively high frequencies [11].

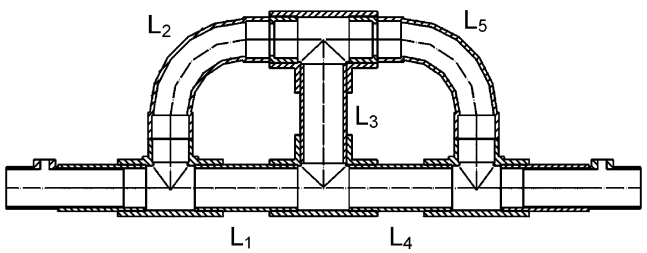

Fig. 2. Scheme of one of the prototypes built with PVC ducts.

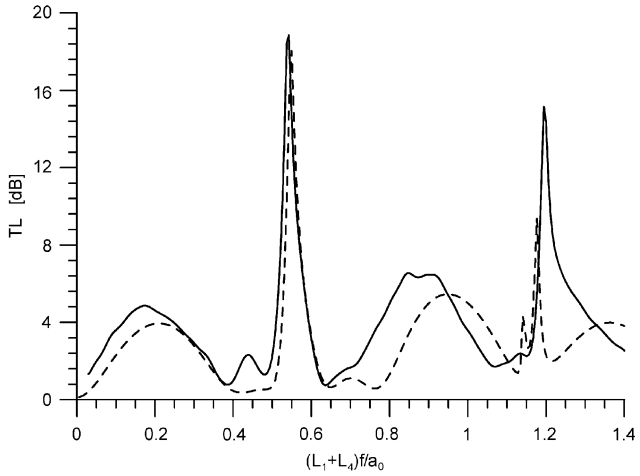

Fig. 3. Comparison between measured (solid line) and computed (dashed line) transmission losses for the system represented in Fig. 2.

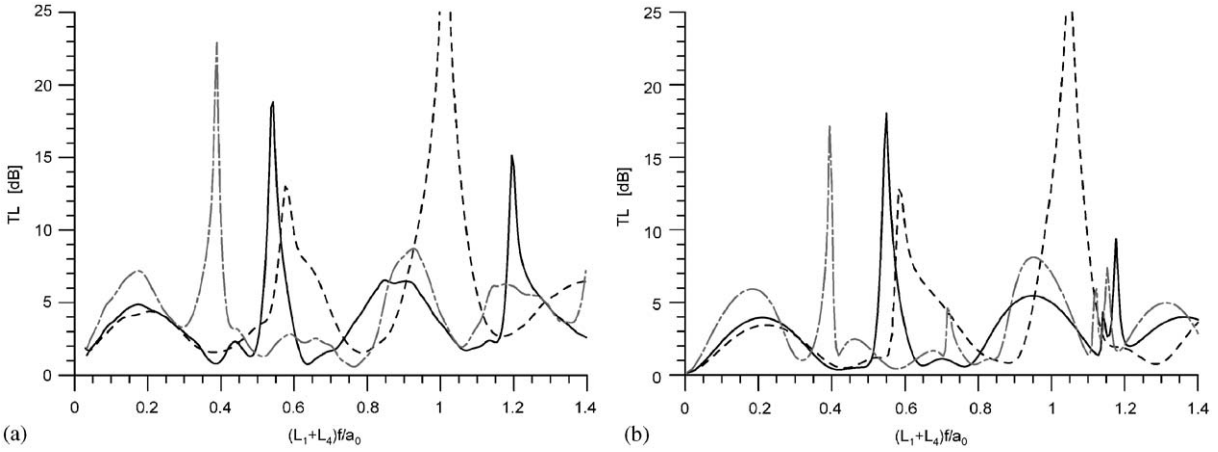

Fig. 4. Transmission Loss of configurations with all diameters equal: $L_1 = L_3 = L_4 = L$, $L_2 = L_5 = \frac{9}{5}L$ (solid line); $L_1 = L_3 = L$, $L_2 = \frac{9}{5}L$, $L_4 = L + L$, $L_5 = \frac{9}{5}L + L$ (dashed line); $L_1 = L_4 = L$, $L_3 = L + L$, $L_2 = L_5 = \frac{9}{5}L + L$ (dash–dot line). (a) Measured, (b) calculated.

Apart from this direct comparison, the ability of the calculation to reproduce changes in the acoustic response due to changes in the system geometry was also evaluated. With this purpose, two different sets of tests were considered. First, the sensitivity to changes in the duct lengths was checked when all the ducts, including the interconnecting pipe, had the same diameter, which was set to 54 mm. Measured results are shown in Fig. 4(a), again as a function of the nondimensional frequency. Apart from the base configuration (same results as in Fig. 3), the TL of a non-symmetric case, where the two ducts at the right of the interconnecting pipe are longer than in the base configuration, has been plotted in dashed line, while a third configuration, in which the

interconnecting pipe and both bended ducts are longer than in the base configuration, has been represented by a dash–dot line.

The corresponding theoretical results are shown in Fig. 4(b). From the comparison between the experimental measurements and the computed results, it is confirmed that the calculation reproduces the main features in the attenuation curves, at least for frequencies at which three-dimensional effects related either with junction geometry or duct curvature are not dominant. Moreover, modifications in the attenuation curves associated with the change in the geometry are properly reproduced. In the two symmetric cases depicted in Fig. 4 (solid line and dash–dot line), there is only one resonance spike for nondimensional frequencies below 1; it can be observed that this resonance shifts to lower frequencies when the difference between the upper and the lower path is increased. However, when a non-symmetric configuration is considered (dashed line), an additional resonance spike appears at a nondimensional frequency of about 1. All these trends are well reproduced by the calculation, as well as the behaviour of the slope of the TL in the very low frequency range.

The second set of tests focused on the influence of the diameter of the interconnecting pipe. Several symmetric prototypes with different interconnecting duct diameters were built and tested in order to assess the sensitivity of the model to modifications in this parameter. The base configuration is the same as for the previous study, i.e. that depicted in Fig. 2, in which the interconnecting pipe has the same diameter as the rest of the ducts. The corresponding measured transmission loss is represented in Fig. 5(a) in solid line, while the dashed line corresponds to a diameter reduction to 4/5 of the original one, and the dash–dot line to a further diameter reduction to half of the original one. It can be seen that a reduction in the interconnecting duct diameter produces a shift to lower frequencies of the first resonance, and for the reduction to half of the original diameter a secondary spike appears at a nondimensional frequency of about 0.6. As it was expected, the calculation matches this trend reasonably, as shown in Fig. 5(b); discrepancies at high frequencies may again be justified by the oversimplified description of the junctions and neglect of the effects of tube curvature in one of the paths of the modified H–Q tube. Even though

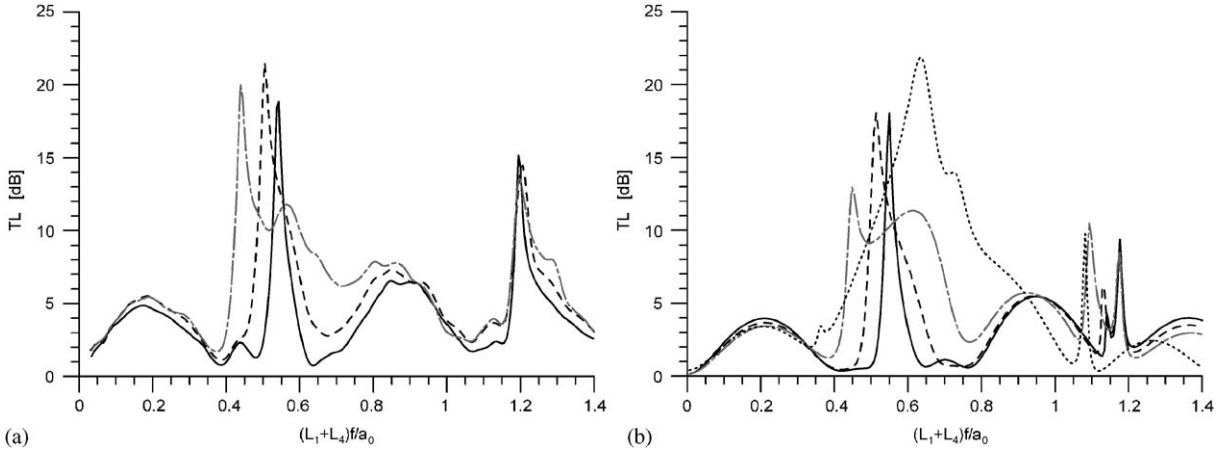

Fig. 5. Transmission loss of configurations with different interconnecting pipe diameter: 54 mm (solid line), 42 mm (dashed line), 27 mm (dash–dot line), 1 mm (dotted line). (a) Measured, (b) calculated.

it was not measured, the limiting case of 1 mm diameter has been added to Fig. 5(b) for reference purposes. It can be observed that, in this case (whose results are virtually identical to those obtained for a simple H–Q tube) the first resonance spike is further shifted to lower frequencies and is now hardly noticeable, while the secondary spike noted above has grown to be the main resonance spike in the system, without any substantial shift in frequency.

4. Discussion of tendencies

While the results discussed in the previous section have provided a limited yet adequate experimental validation of the theoretical analysis presented, they also make evident the non-trivial influence of the interconnecting pipe on the acoustic behaviour of the system, and thus the necessity of analysis techniques that may provide more information than the mere comparison of transmission loss curves.

In order to get a global view of the influence of the intermediate pipe on the transmission loss of the system, the analysis was performed by means of transmission loss contour plots, extending the approach used in Ref. [5] for the simple H–Q tube. On these plots, the main tendencies were identified and interpreted in relatively simple terms, as shown in the following.

Given the huge number of characteristic parameters of the modified H–Q tube, and trying to focus on the influence of the interconnecting pipe and on potential practical implementations, only the particular cases with $S_1 = S_2 = S_4 = S_5 = S$ and $L_1 = L_4 = L$ were considered; S was set to $20.4\,\mathrm{cm}^2$ and L was set to 200 mm.The additional restriction $L_2 = L_5 = (L_2/L_1)L$ was imposed in order to allow comparison with the contours obtained for the simple H–Q tube. In this way, only the length and cross section of duct 3 (the interconnecting pipe) were varied.

As it was suggested by the results discussed in the previous section, the behaviour of the H–Q tube modified with an interconnecting pipe is rather complex and, in principle, one may not expect to find simple relationships for the resonance spikes as those presented by Selamet et al. [3] for the simple H–Q tube. However, the analysis of the transmission loss contours allowed the identification of the main issues.

In Fig. 6 transmission loss contours for values of L_2/L_1 (i.e. L_2/L) ranging from 0.01 to 4, with different interconnecting pipe diameters, have been depicted, showing the clear influence of this diameter on the general behaviour of the system. The length of the interconnecting pipe was set to 200 mm. In Fig. 6(a), several resonance frequencies have been highlighted with an ellipse; it can be observed that when the interconnecting pipe diameter is increased these highlighted attenuation spikes are smaller (see Figs. 6(b) and (c)), finally disappearing if the area is sufficiently increased, as in Fig. 6(d). The rest of the resonance spikes have different shapes for different diameters, but nevertheless their respective midpoints remain unaffected.

This relatively well ordered pattern, when compared with the results of transmission loss contours for a simple H–Q tube shown in Ref. [5], suggested that, as a first approximation, the features observed could be attributed to the combined effect of different interferential paths (i.e. simple H–Q tubes). With the geometrical restrictions considered, a careful analysis of the modified H–Q tube allowed the identification of only three such interferential paths. In Fig. 7 these interferential paths, denoted in the following as IP1, IP2 and IP3, have been plotted. Needless to say that it should not be expected that the behaviour of the total system is the crude addition of

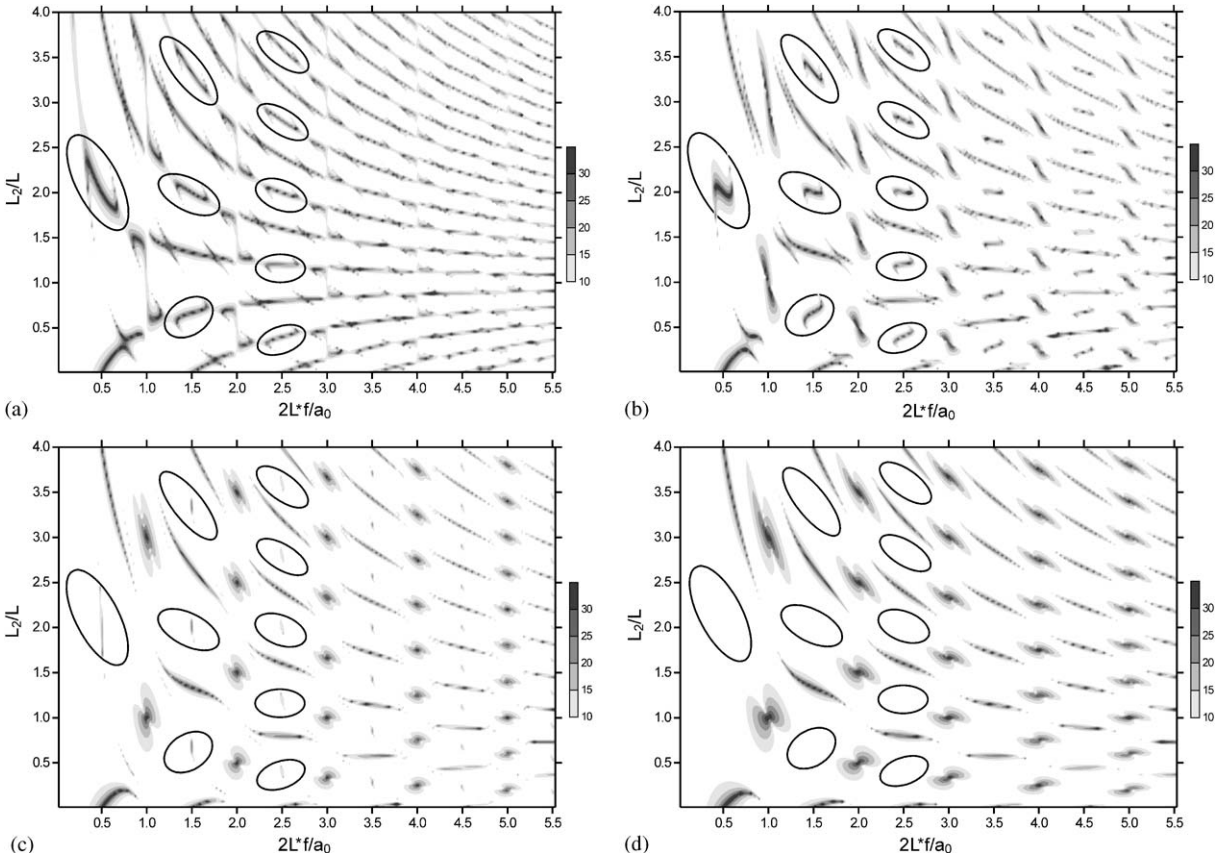

Fig. 6. TL contours with $L_3 = L_1$, (a) $D_3 = D_1/4$, (b) $D_3 = D_1/2$, (c) $D_3 = D_1$, (d) $D_3 = 3D_1/2$.

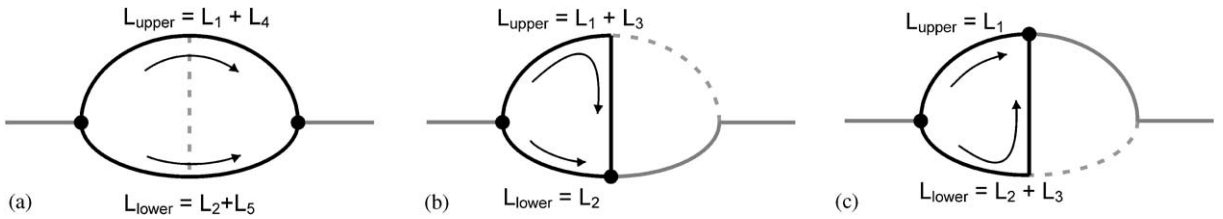

Fig. 7. Possible interferential paths, (a) IP1, (b) IP2, (c) IP3.

the three interferential paths; however, it will be shown below that their general trends allow interpretation of the most relevant tendencies found in the transmission loss.

As pointed out by Selamet et al. [3] the resonance locations for a H–Q tube, according to the notation in Fig. 7(a) , are given by

$$\frac{\sin(kL_{\text{upper}})}{\sin(kL_{\text{lower}})} = -\frac{S_{\text{upper}}}{S_{\text{lower}}}. \tag{11}$$

In the particular case that $S_{upper} = S_{lower}$, Eq. (11) simplifies to give

$$k\left|L_{upper} - L_{lower}\right| = (2n-1)\pi, \quad n = 1, 2, \ldots, \tag{12}$$

$$k\left(L_{upper} + L_{lower}\right) = 2m\pi, \quad m = 1, 2, \ldots, \tag{13}$$

this is, two different families of resonance spikes: Eq. (12) gives the locations for transmission loss spikes of type I and Eq. (13) for spikes of type II [3].

These equations, which hold for a two-duct interferential path, were applied to the three relevant interferential paths identified in the modified H–Q tube, as defined above. While IP1 is, with the geometrical restrictions considered, a simple H–Q tube, the application of such description to IP2 and IP3 is indeed doubtful, since they are not exactly simple H–Q tubes: with any of the configurations considered, a branch of IP2 would consist of two ducts of different diameters connected by a sudden area change since, as noted above, the diameter of the interconnecting pipe is different from the rest. The same occurs with one of the branches of IP3. However, as a first approximation to the problem it was initially assumed that the effect of this area change could be neglected, so that the area ratio in Eq. (11) is equal to unity and Eqs. (12) and (13) can thus be applied to IP2 and IP3.

Two significant cases, corresponding to the smallest and the largest interconnecting pipe diameter, will be considered in detail. First, the case $L_3 = L_1$ and $D_3 = D_1/4$ (Fig. 6(a)), will be discussed. In this case, IP1 is expected to be the main feature governing the acoustic response of the system, since the diameter of the interconnecting pipe is small in comparison with the common diameter. Therefore, the transmission loss contour is essentially determined by the resonance frequencies of IP1, being very similar to a simple H–Q tube.

Appling Eqs. (12) and (13) to IP1, IP2 and IP3 one obtains the equations listed in Table 1, where $\xi_x = (L_1 + L_4)f/a_0 = 2L_1 f/a_0$, $\xi_y = L_2/L_1$, and $n = 1,2,\ldots$. Results for this first case are represented in Fig. 8. Together with the TL contour, the IP1-type I curves (solid line) and IP1-type II curves (dashed line), are plotted in Fig. 8(a). It can be observed that resonance spikes are located at the same position as the theoretical curves given by IP1-type I, whereas the curves associated with IP1-type II only induce resonance spikes close to the crossing points of both series types.

In Fig. 8(b), the IP2-type I curves (solid line) and IP3-type I curves (dashed line) have been plotted. It can be seen that those points which, from Fig. 8(a), show deviations from the behaviour of a simple H–Q tube (i.e. IP1), are located around the crossing points of the two curves

Table 1
Approximate theoretical curves for a symmetric modified H–Q tube

	Type I	Type II
Interferential path 1	$\xi_y = 1 \pm (2n-1)/(2\xi_x)$	$\xi_y = n/\xi_x - 1$
Interferential path 2	$\xi_y = 1 + L_3/L_1 \pm (2n-1)/\xi_x$	$\xi_y = 2n/\xi_x - 1 - L_3/L_1$
Interferential path 3	$\xi_y = 1 - L_3/L_1 \pm (2n-1)/\xi_x$	Same as IP2-type II

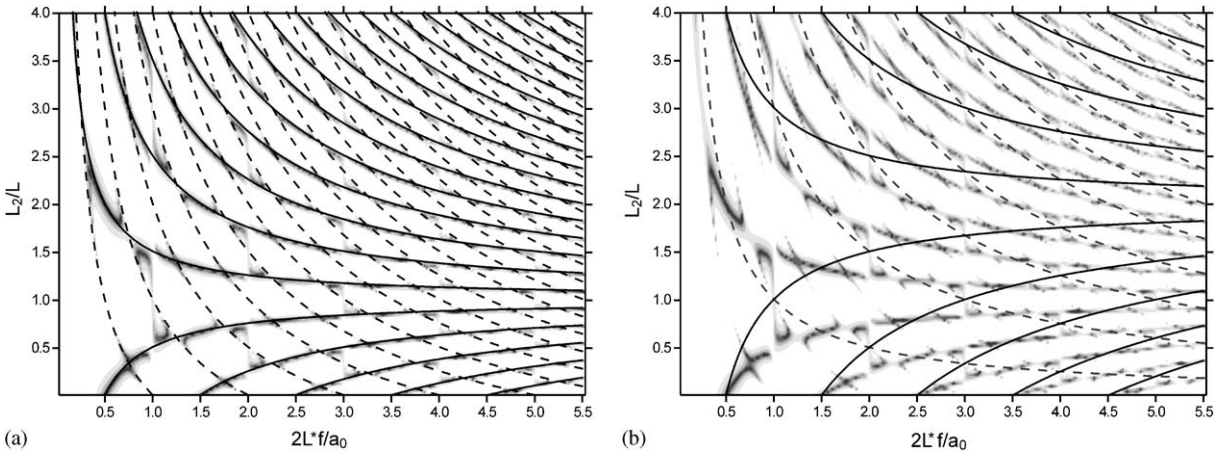

Fig. 8. Symmetric modified H–Q tube with $L_3 = L_1$ and $D_3 = D_1/4$: transmission loss contour with superimposed theoretical lines. (a) IP1-type I curve (solid line) and IP1-type II curve (dashed line); (b) IP2-type I curve (solid line) and IP3-type I curve (dashed line).

represented, so that IP2 and IP3 give an indication of the effect of the interconnecting duct, even though their consideration in terms of simple H–Q tubes is a rather crude approximation.

The second relevant case considered was that with $D_3 = 3D_1/3$. Now, two families of resonance frequencies may be distinguished in the corresponding transmission loss results, shown in Fig. 6(d). Those of the first family will be referred to as "spread" resonances due to their appearance, and those of the second family will be denoted as "lobe" resonances, as they consist of a central point with two adjacent oval areas.

In Fig. 9(a) the corresponding TL contour is represented, together with the theoretical curves of IP1, type I (solid line) and type II (dashed line), and the curves of IP2-type II (dash–dot line). With the simplification assumed for IP2 and IP3, the equations to be used are again those shown in Table 1. It is clear from this figure that the two groups of curves related to IP1 are not sufficient to describe the transmission loss contour, as could be expected. Nevertheless, it is also clear that spread resonances lie on the attenuation spike locations of IP1 that have remained effective when increasing the interconnecting pipe diameter, even though their endpoints appear to have turned toward the crossing points between IP1-type II and IP2-type II curves.

The midpoint of both types of resonances can be found from the crossing points of type I curves, as shown in Fig. 9(b). Spread resonances are centred at the crossing points between IP1-type I curves (solid line) and IP2-type I curves (dashed line). Lobe resonances centre points lie on the intersection of IP2-type I curves with IP3-type I curves (dash–dot line). The other crossing points of type I curves, between IP1 and IP3, are not centre points of any attenuation spikes because a type II curve (corresponding to IP2, and plotted with dotted line) passes through. These last points were precisely the midpoints of the resonances that vanished when the intermediate pipe diameter was increased.

The previous results indicate that, even though the assumption that IP2 and IP3 may be calculated with Eqs. (12) and (13) may be regarded as crude, most of the features observed in the behaviour of the modified H–Q tube are explained in relatively simple terms. However, one might

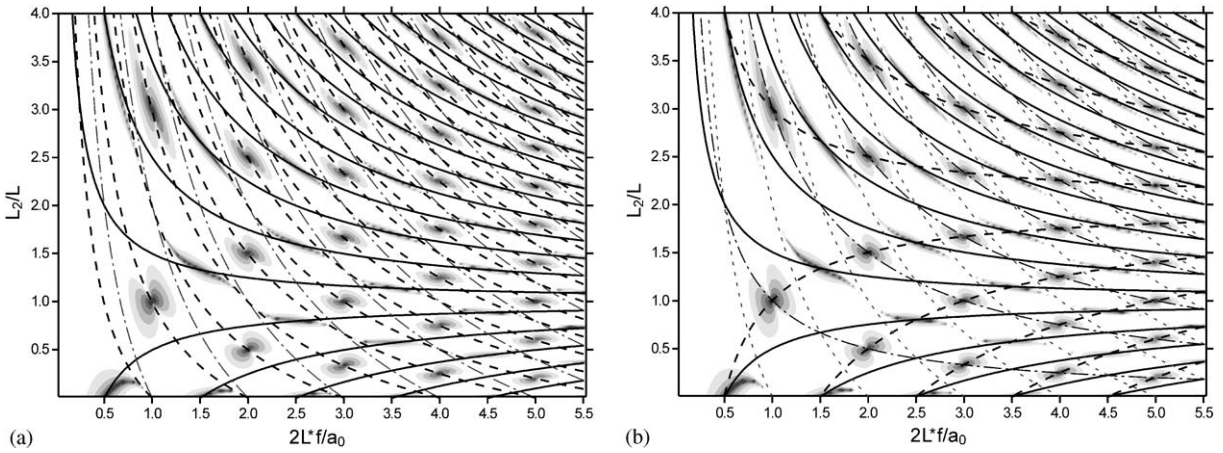

Fig. 9. Symmetric modified H–Q tube with $L_3 = L_1$ and $D_3 = 3D_1/2$: Transmission loss contour with superimposed theoretical lines. (a) IP1-type I curve (solid line), IP1-type II curve (dashed line) and IP2-type II curve (dash–dot line); (b) IP1-type I curve (solid line), IP2-type I curve (dashed line), IP2-type II curve (dotted line) and IP3-type I curve (dash–dot line).

think of another simplified approach, in which the ingredient of the differences in diameter is approximately incorporated into the analysis. In this approach, the diameter of the interconnecting pipe was used for the entire branch containing it, so that the two branches of each interferential path have different diameters and, as a result, the resonance frequencies of IP2 and IP3 must be obtained by solving Eq. (11).

The transmission loss contour for $D_3 = 3D_1/2$ has been plotted in Fig. 10(a), together with the curves calculated with Eq. (11) for IP2 (solid line) and IP3 (dashed line), and also with IP1-type I curves (dash–dot line). It can be observed that the shape of the spread resonances is reproduced in a very accurate way; moreover, every centre point of both types of attenuation spikes was located. Therefore, even though this is also an approximate solution, the consideration of the difference in cross-section produces a more accurate description of the acoustic behaviour of the system.

In order to highlight the relationship between both approximations and to provide some basis for the ''equal-area'' approach, the solution of Eq. (11) for IP2 will now be considered in some detail. Since this equation does not admit an explicit solution, it is convenient to define an auxiliary magnitude ξ_z , as

$$\xi_z = \sin(\pi\xi_x\xi_y) + (D_1/D_3)^2 \sin(\pi\xi_x(1 + L_3/L_1)), \tag{14}$$

so that the solution to Eq. (11) corresponds to $\xi_z = 0$, as can be readily verified making use of the definitions of ξ_z, and ξ_y. Fig. 10(b) shows lines with $\xi_z = 0$, for the case $L_3 = L_1$ and with different interconnecting pipe diameters. For reference, the values corresponding to the case when $D_1 = D_3$ are represented by areas: $\xi_z <$ with a white surface, and $\xi_z > 0$ with a shaded surface, so that in this particular case the condition $\xi_z = 0$ is represented by the contact lines between both areas, thus giving the location of types I and II attenuation spikes of IP2. The continuous character of these limiting lines is actually only apparent and is a particular feature of the case considered ($D_1 = D_3$),

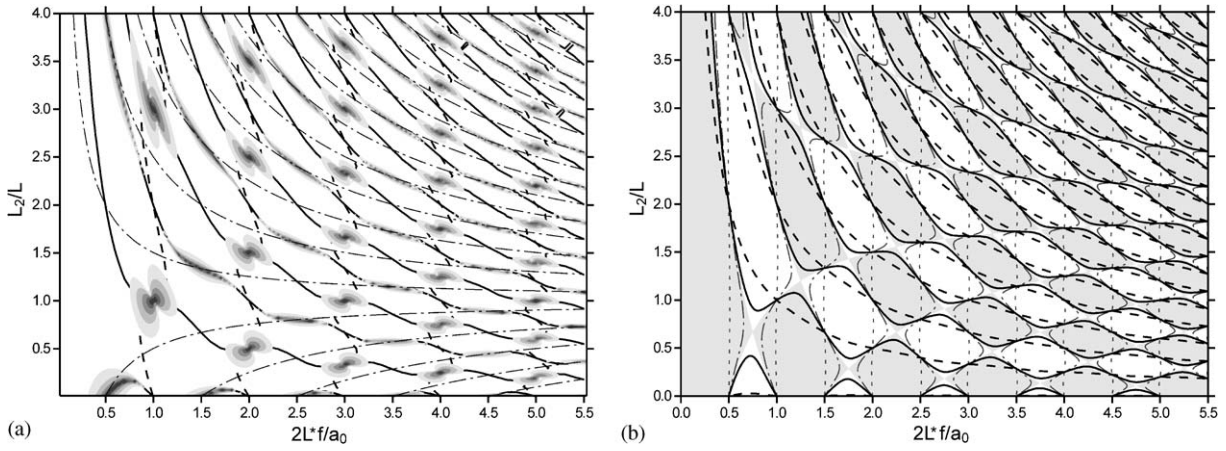

Fig. 10. Interferential paths with area ratio different from 1: (a) TL contour of a symmetric modified H–Q tube with $L_3 = L_1$ and $D_3 = 3D_1/2$, together with IP2 curves (solid line), IP3 curves (dashed line) and IP1-type I curves (dash–dot line); (b) Solution of Eq. (11) for the interferential path IP2: $D_3 = 1.1D_1$ (solid line), $D_1 = 1.1D_3$ (dash–dot line), $D_3 = 4D_1$ (dashed line) and $D_1 = 4D_3$ (dotted line).

as can be readily verified by slightly modifying the diameter ratio. Consider, for instance, the case $D_3 = 1.1D_1$; the corresponding $\xi_z = 0$ curves (solid line) reveal an unexpected behaviour, since curves that seemed to be independent in the case $D_1 = D_3$ are now connected, showing a smooth behaviour. Considering an opposite modification ($D_1 = 1.1D_3$) the same behaviour is observed for the corresponding $\xi_z = 0$ curves (dash–dot line), but now on a different family of curves.

If instead of a slight modification a major change is introduced, one finds that the $\xi_z = 0$ curves tend to simple asymptotic forms. The cases represented in Fig. 10(b) illustrating this behaviour correspond to $D_3 = 4D_1$ (dashed line) and $D_1 = 4D_3$ (dotted line). In any case, the solution corresponding to $D_1 = D_3$ still provides information relevant for the proper location of the resonance spikes, which further supports the otherwise crude approximation used.

5. Summary and conclusions

A transfer matrix for a Herschel–Quincke (H–Q) tube modified with an interconnecting pipe has been developed. First, a general solution for two arbitrary interconnected branches was obtained, and the consistency of the result was checked in the two limiting cases of a simple interferential system and two interferential systems in series. Then, the results were particularized to the case in which all the branches considered were uniform ducts, thus obtaining the transfer matrix of the modified H–Q tube.

Several prototypes were built and their attenuation characteristics measured with a modified impulse method. The results showed good agreement with the transmission loss computed from the transfer matrix model, thus indicating the possibility to explore the main features of the acoustic behaviour of the system via the model.

Transmission loss contour maps for several relevant configurations were studied, focusing on the influence of the diameter of the interconnecting pipe. This study revealed the possibility of describing the main features of the system by considering the joint action of three simple interference paths, whose characteristics were approximated in two different ways to allow for the use of simple H–Q tube relationships. With this approach, it has been possible to predict the existence of any resonance spike from relatively simple relationships, thus providing a useful tool for the potential exploitation of this system as a practical attenuation device.

Acknowledgement

This research was partially supported by Ministerio de Ciencia y Tecnología under Grant DPI2000-0743-C02-02.

Appendix

Both limiting cases indicated in section 2 are addressed by setting

$$\begin{bmatrix} A_3 & B_3 \\ C_3 & D_3 \end{bmatrix} = \begin{bmatrix} 1 & R \\ 0 & 1 \end{bmatrix}, \tag{A.1}$$

where R is a convenient acoustic resistance, so that indeterminations in the terms defined in Eq. (6) are avoided. The first case of two interferential systems in series is then obtained taking $R \to 0$. In this way, branch number three is represented by an identity matrix and then, the outlet of branches 1 and 2 and the inlet of branches 4 and 5 collapse at the same point. Therefore, substituting Eqs. (A.1) into Eq. (6), from Eq. (5) one obtains, after setting $R \to 0$, the following expressions:

$$\begin{aligned}
m &= (D_1 B_2 + B_1 D_2)\frac{B_4 + B_5}{B_5(B_1 + B_2)}, \\
n &= B_1 B_2 \frac{B_4 + B_5}{B_5(B_1 + B_2)}, \\
t &= A_4 + \frac{A_5 B_4}{B_5}, \\
x &= \frac{(D_1 - D_2)(A_1 - A_2)}{(B_1 + B_2)} + \frac{(D_4 - D_5)(B_1 D_2 + D_1 B_2)}{B_5(B_1 + B_2)} - C_1 - C_2, \\
y &= \frac{B_1(B_5 A_2 + B_2 D_5) + B_2(B_5 A_1 - B_1 D_4)}{B_5(B_1 + B_2)}, \\
z &= C_4 + \frac{A_5 D_4 - 1}{B_5}.
\end{aligned} \tag{A.2}$$

Eqs. (A.2), when substituted into Eq. (7), lead to a transfer matrix that may be written as the product of the transfer matrices of two simple interferential systems, as given in Ref. [5]. In the simple case of two H–Q tubes in series an explicit expression for the resulting transfer matrix is obtained. All the transfer matrices involved are given by Eq. (8). Now, for simplicity in

the notation define

$$\Phi_j = \frac{\phi_j}{2\alpha_j}, \quad \Theta_j = \frac{a_0}{2\alpha_j S_j}. \tag{A.3}$$

Then, combining Eqs. (7), (8), (A.2) and (A.3), and after some algebra, one obtains the four-pole parameters as

$$\begin{aligned}
A &= \frac{\Phi_1\Theta_2 + \Theta_1\Phi_2}{\Theta_1 + \Theta_2}\frac{\Phi_4\Theta_5 + \Theta_4\Phi_5}{\Theta_4 + \Theta_5} + \frac{\Theta_1\Theta_2}{\Theta_1 + \Theta_2}\left(\frac{\Theta_4 S_4^2 + \Theta_5 S_5^2}{a_0^2} - \frac{(\Phi_5 - \Phi_4)^2}{\Theta_4 + \Theta_5}\right),\\
B &= \frac{\Theta_1\Theta_2\Theta_4\Theta_5}{(\Theta_1 + \Theta_2)(\Theta_4 + \Theta_5)} \cdot \left(\frac{\Phi_1}{\Theta_1} + \frac{\Phi_2}{\Theta_2} + \frac{\Phi_4}{\Theta_4} + \frac{\Phi_5}{\Theta_5}\right),\\
C &= \left(\frac{\Theta_1 S_1^2 + \Theta_2 S_2^2}{a_0^2} - \frac{(\Phi_2 - \Phi_1)^2}{\Theta_1 + \Theta_2}\right)\frac{\Phi_4\Theta_5 + \Theta_4\Phi_5}{\Theta_4 + \Theta_5} + \frac{\Phi_1\Theta_2 + \Theta_1\Phi_1}{\Theta_1 + \Theta_2}\left(\frac{\Theta_4 S_4^2 + \Theta_5 S_5^2}{a_0^2} - \frac{(\Phi_5 - \Phi_4)^2}{\Theta_4 + \Theta_5}\right),\\
D &= \left(\frac{\Theta_1 S_1^2 + \Theta_2 S_2^2}{a_0^2} - \frac{(\Phi_2 - \Phi_1)^2}{\Theta_1 + \Theta_2}\right)\frac{\Theta_4\Theta_5}{\Theta_4 + \Theta_5} + \frac{\Phi_1\Theta_2 + \Theta_1\Phi_2}{\Theta_1 + \Theta_2}\frac{\Phi_4\Theta_5 + \Theta_4\Phi_5}{\Theta_4 + \Theta_5}.
\end{aligned} \tag{A.4}$$

This expression may be obtained by multiplying two H–Q tube transfer matrices, as defined in Ref. [3].

The second case, i.e. a simple interferential system, is obtained by taking $R \to \infty$. In this way, wave propagation through the connecting branch is not allowed and thus the connection between the branches disappears. By following the same procedure as in the first case, but now using $R \to \infty$ the following expressions are reached:

$$\begin{aligned}
m &= D_1 + \frac{B_1(B_5C_2 + D_5D_2) + B_4}{B_5A_2 + D_5B_2},\\
n &= B_1,\\
t &= \frac{1}{B_5}\left(B_5A_4 + A_5B_4 + \frac{B_5B_1 - B_4B_2}{B_5A_2 + D_5B_2}\right),\\
x &= \frac{D_4 - A_1(B_5C_2 + D_5D_2)}{B_5A_2 + D_5B_2} - C_1,\\
y &= A_1,\\
z &= \frac{1}{B_5}\left(B_5C_4 + A_5D_4 - \frac{B_5A_1 + D_4B_2}{B_5A_2 + D_5B_2}\right)
\end{aligned} \tag{A.5}$$

Combining Eqs. (7), (8), (A.3) and (A.5), with the additional restriction that sections of branches 1 and 4 are equal, $S_1 = S_4$, and the same for branches 2 and 5, $S_2 = S_5$, after some algebra one gets

$$\begin{aligned}
A = D &= \frac{\Phi_{1+4}\Theta_{2+5} + \Theta_{1+4}\Phi_{2+5}}{\Theta_{1+4} + \Theta_{2+5}},\\
B &= \frac{\Theta_{1+4}\Theta_{2+5}}{\Theta_{1+4} + \Theta_{2+5}},\\
C &= \frac{\Theta_{1+4}S_1^2 + \Theta_{2+5}S_2^2}{a_0^2} - \frac{(\Phi_{2+5} - \Phi_{1+4})^2}{\Theta_{1+4} + \Theta_{2+5}}.
\end{aligned} \tag{A.6}$$

Here, Φ_{i+j} and Θ_{i+j} refer to the magnitudes defined in Eq. (A.3) for a duct with length $l_i + l_j$. The transfer matrix obtained is equivalent to the expression for the particular case of a simple H–Q tube given by Selamet et al. [3].

References

[1] J.F.W. Herschel, On the absorption of light by coloured media, viewed in connection with the undulatory theory, *Philosophical Magazine* 3 (1833) 401–412.
[2] G. Quincke, Über Interferenzapparate für Schallwellen, *Annalen der Physik und Chemie* 128 (1866) 177–192.
[3] A. Selamet, N.S. Dickey, J.M. Novak, The Herschel–Quincke tube: a theoretical, computational, and experimental investigation, *Journal of the Acoustical Society of America* 96 (1994) 3177–3185.
[4] A. Selamet, V. Easwaran, Modified Herschel–Quincke tube: attenuation and resonance for n-duct configuration, *Journal of the Acoustical Society of America* 102 (1997) 164–169.
[5] A.J. Torregrosa, A. Broatch, R. Payri, A study of the influence of mean flow on the acoustic performance of Herschel–Quincke tubes, *Journal of the Acoustical Society of America* 107 (2000) 1874–1879.
[6] Z. Zhichi, L. Song, T. Rui, G. Rui, D. Genhua, L. Peizi, Application of Quincke tubes to flow ducts as a sound attenuation device, *Noise Control Engineering Journal* 46 (1998) 245–255.
[7] J.Y. Ha, K.J. Kim, Analysis of MIMO mechanical systems using the vectorial four pole parameter method, *Journal of Sound and Vibration* 180 (1995) 333–350.
[8] V.H. Gupta, On independence of reciprocity, symmetry and conservativeness of one-dimensional linear systems, *Journal of Sound and Vibration* 179 (1995) 547–552.
[9] M.L. Munjal, *Acoustics of Ducts and Mufflers*, Wiley, New York, 1987.
[10] F. Payri, J.M. Desantes, A. Broatch, Modified impulse method for the measurement of the frequency response of acoustic filters to weakly nonlinear transient excitations, *Journal of the Acoustical Society of America* 107 (2000) 731–738.
[11] S. Félix, V. Pagneux, Sound propagation in rigid bends: a multimodal approach, *Journal of the Acoustical Society of America* 110 (2001) 1329–1337.